Multi-Scale Characterization of Orthotropic Microstructures

M.A. Tschopp[1,2], G.B. Wilks[1,3], J.E. Spowart[1]

[1] Air Force Research Laboratory, Materials and Manufacturing Directorate, Wright-Patterson Air Force Base, OH 45433, USA
[2] Universal Technology Corporation, Dayton, OH
[3] General Dynamics Inc., Dayton, OH

E-mail: mark.tschopp.ctr@wpafb.af.mil

Abstract.

Computer generated 2D microstructures of varying second-phase area fraction (5%-30%), aspect ratio (1-16), and degree of alignment (where the reinforcement major-axis orientation is random, perfectly aligned, or semi-aligned) are analyzed via the isotropic and directional forms of the computationally efficient Multi-Scale Analysis of Area Fractions (MSAAF) technique. The impact of these microstructure parameters on the representative volume element (RVE) necessary to characterize a microstructure is ascertained with variations in isotropic and directional homogenous length scales, derivative quantities of the MSAAF technique. Analysis of these results produces empirical expressions for the directional homogenous length scale as a function of area fraction and aspect ratio for the limiting cases of random and "perfect" second phase alignment. Generally, particle alignment is observed to increase the aspect ratio of a microstructure's RVE - a trend amplified by higher reinforcement aspect ratios and lower area fractions. Particle alignment also decreases the absolute size of such an element by reducing the directional homogenous length scales transverse to the axis of alignment. Periodic boundary conditions on the perimeter of the synthetic microstructures are used to characterize the error in the MSAAF technique via multiple instantiations of the same microstructure, which further indicates that the statistical variation in linear fraction measured using the directional technique error in the directional homogenous length scale can be an order of magnitude less than that measured by the isotropic technique homogenous length scale at the same length scale.

Submitted to: *Modelling Simulation Mater. Sci. Eng.*

1. Introduction

When assessing structure-property relationships for various materials, it is necessary to define a representative length scale or volume element for characterization or simulation to avoid misleading predictions of macroscopic deformation, fracture, or transport behavior. Likewise, a model or material sample must have sufficient resolution to capture the phenomena of interest. Ideally, a component-sized material model or sample should have the highest resolution possible; however, practical limitations on experimental and computational resources bound the extent and resolution of material models.

The balance between these two often competing needs of extent and resolution has been an underlying theme of numerous studies regarding characterization of heterogeneous materials. Researchers have focused on developing techniques for determining representative length scales for the extent of microstructures based on area fraction or volume fraction [1, 2, 3, 4]; such approaches have shown sensitivity to microstructure clustering and, in fact, are excellent metrics for characterizing this property. The inverse problem of segmenting a microstructure to varying length scales (homogenizing) has also been pursued as a route for identifying the critical length scale at which macroscopic properties are controlled by shorter length scale features; these features are often associated with second phase clustering, its absence, or contribution to percolation [5, 6, 7, 8]. In fact, recent advances in multiscale modeling have emerged due to the ability to homogenize some regions while considering the local behavior in others; such techniques incorporate various length scales associated with the microstructure and its local properties in their formulation [9, 10].

The correlation between critical length scales in the microstructure and the inherent mechanical behavior of heterogeneous microstructures has been examined in numerous computational and experimental studies. For example, Spowart [11] predicted that clustering of reinforcement particles in an Al-27.5%SiC metal matrix composite has a noticeable effect on the yield strength and an even stronger effect on strain-hardening, even though the same level of clustering has only a weak effect on the elastic modulus. These results indicate that each aspect of mechanical behavior is controlled by a different representative length scale in the microstructure and, consequently, that representative volume elements (RVEs) of increasing size were necessary to characterize elastic modulus, yield strength, and strain-hardening, respectively. Additionally, Borbèly *et al.* [2] measured the local volume fractions in an Al-20%Al_2O_3 metal-matrix composite through 3D microtomography to define a microstructure correlation length and, hence, a geometric RVE for this material. Further simulations of elastic and plastic behavior with various window sizes showed that the RVE necessary to obtain accurate effective plastic properties was approximately twice the size of the RVE needed to obtain equally accurate effective elastic properties. Moreover, the influence of second phase distribution on damage accumulation and fracture has also been characterized by numerous authors in various materials, *e.g.*, [12, 13, 14]. In their seminal work on crack deflection around second phase inclusions in a brittle matrix, Faber and Evans

analyzed and experimentally verified that a clustered second phase distribution – as defined by a divergence from a uniform distribution for a given volume fraction – significantly increased fracture resistance in ceramic matrix composites by increasing the degree of crack deflection and crack twist [12, 13]. The clustering of particles is associated with a critical length scale for fracture. In experiments relating to ductile fracture, Wilks analyzed second phase inclusions in a ductile matrix and found that deformation processing decreased the size of the RVE in an Al-25%SiC composite; the smaller RVE correlated with (i) an increase in interparticle separation due to cluster breakdown, (ii) a larger length scale with respect to the ductile fracture process, and (iii) a substantial increase in fracture toughness [14]. Finite element simulations of microstructure domains reconstructed from experimental images of multiphase materials have also provided insight into plasticity, damage evolution, and the fracture process [15, 16, 17, 18, 19]. In all of these experiments and simulations, the length scale of the underlying microstructure plays a commanding role in the mechanical behavior of the material.

Therefore, it is important to have a consistent methodology for characterizing the critical length scales within heterogeneous materials. The focus of this work is the effect of second-phase anisotropy on critical length scales and the corresponding RVE size. Orthotropic (aligned) microstructures are very common in materials where deformation processing has been imposed or directional synthesis routes have been pursued [14]. These microstructures constitute a sound basis for analyzing limiting bounds on anisotropic length scale effects. Moreover, such microstructures represent a basis for analyzing microstructures with several preferred directions of alignment (*e.g.*, precipitated microstructures with preferred orientation relationships), or more generalized anisotropy. In this work, we investigate the interaction between length-scale effects and second phase orthotropy through applying the isotropic and directional forms of the Multi-Scale Analysis of Area Fractions (MSAAF) technique [1, 20] to computer-generated two-dimensional microstructure images containing ellipsoidal particles of varying aspect ratio, area fraction, and propensity for alignment.

2. Methodology

2.1. Synthetic microstructure conditions

Synthetic microstructures were generated with the factors and factor levels summarized in Table 1. The four area fractions (A_f) and five aspect ratios (AR) were chosen to give a wide range and sufficiently resolved gradient in microstructure characteristics for the subsequent analyses. The orientation distributions studied include limiting conditions where all particles are aligned vertically (90°), all particles are randomly oriented (Random), and an intermediary factor level ($90° \pm 20°$) that reflects orientations normally distributed about 90° with a standard deviation of 20°. In all, 60 distinct synthetic microstructures (conditions) were studied corresponding to the permutation

Table 1. The test matrix for these simulations.

Factor	Factor Levels				
Volume Fraction	5%	10%	20%	30%	
Aspect Ratio	1	2	4	8	16
Orientation Distribution	90°	$90° \pm 20°$	Random		

of these factors.

2.2. Synthetic microstructure generation

Each synthetic microstructure condition was generated via a simple procedure, similar to the Random Sequential Adsorption (RSA) technique, *e.g.*, [21, 22]. First, particle dimensions (in pixels‡) were calculated for each aspect ratio along with the number of particles necessary to obtain the prescribed area fraction. In order to mitigate any unintended effect of particle size distribution, particle size (area) was kept constant through successively higher area fractions; the details of this effect will be considered in future work as a subset of the more general interaction of microstructure anisotropy and particle polydispersivity. Particle orientation was then randomly sampled from the predetermined orientation distribution while the coordinates of the particle centroid were selected via a random number generator. The influence of boundary effects on particle placement was mitigated by imposing periodic boundary conditions on the vertical and horizontal edges of the microstructure domain; particles that extend beyond the image bounds were wrapped back onto the opposite side of the image. Analytic criteria were used to reject overlapping particles. Particle placement proceeded until the specified area fraction was obtained. Resulting microstructures contained a minimum of 4,000 particles and were of 4,096 x 4,096 pixels in extent.

Sample regions from each synthetic microstructure condition as a function of AR and A_f are depicted in Fig. 2.2. The general influence of each considered orientation distribution on a high area fraction ($A_f = 30\%$), high aspect ratio ($AR = 16$) microstructure is shown in Fig. 2. Notice in these two figures that particles with similar orientations cluster at higher area fractions and aspect ratios. This effect can be correlated with the variation in jamming threshold [23] for such microstructures and indicates that the distribution of particle centroids may not be truly random, due to the stochastic nature of particle placement.

2.3. Multi-Scale Characterization

2.3.1. Isotropic Microstructures The homogenous length scale (L_H) was developed to determine a representative length scale for a particular microstructure based on the variations in area fraction of a second phase as a function of length scale (Q)

‡ In these synthetic microstructures, absolute length scale is arbitrary; since features dimensioned in pixels may seem unphysical, the reader may wish to consider a scale of 1 pixel = 1 μm.

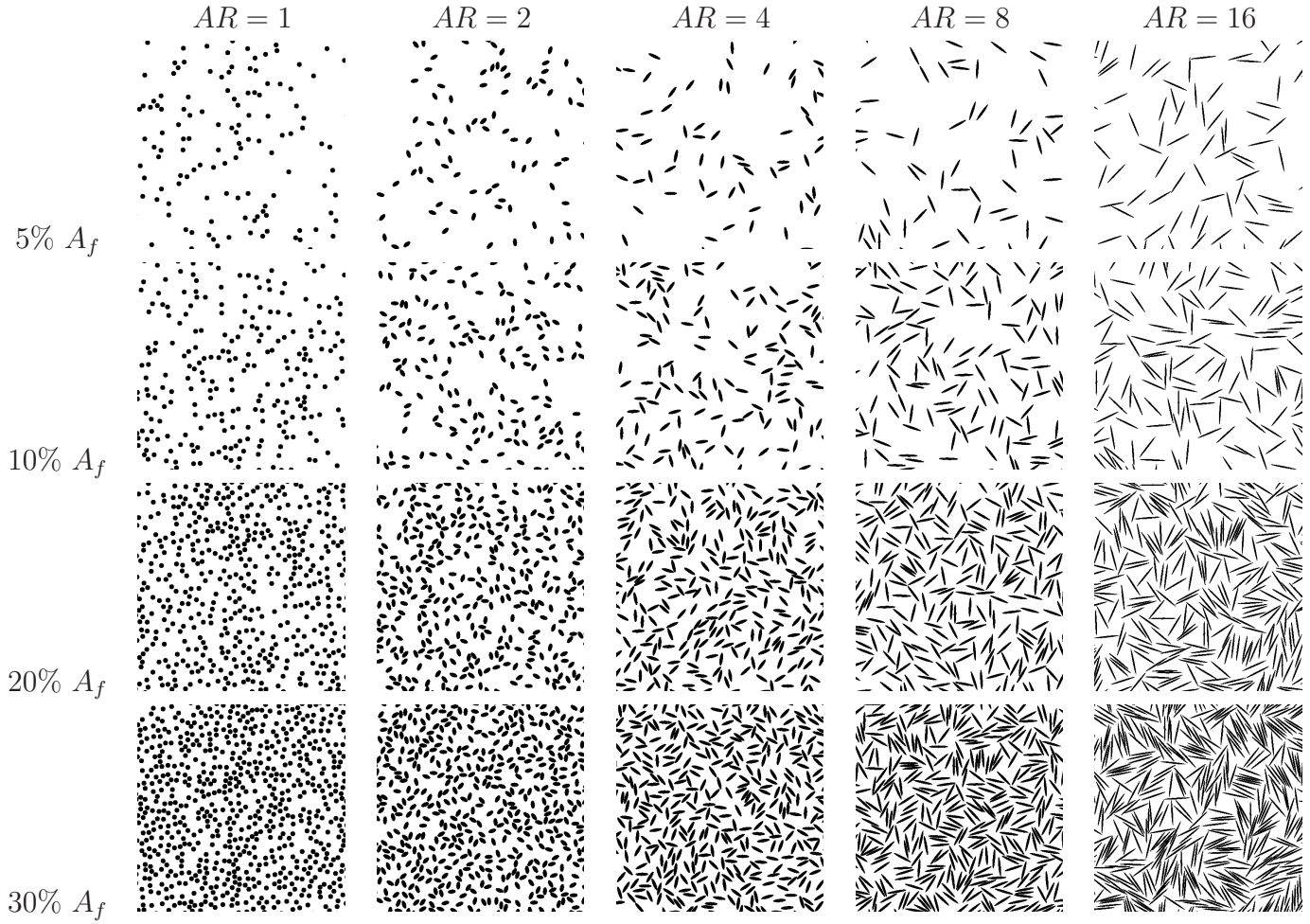

Figure 1. All synthetic microstructure conditions for randomly oriented particles displayed as a function of aspect ratio (AR) and area fraction (A_f).

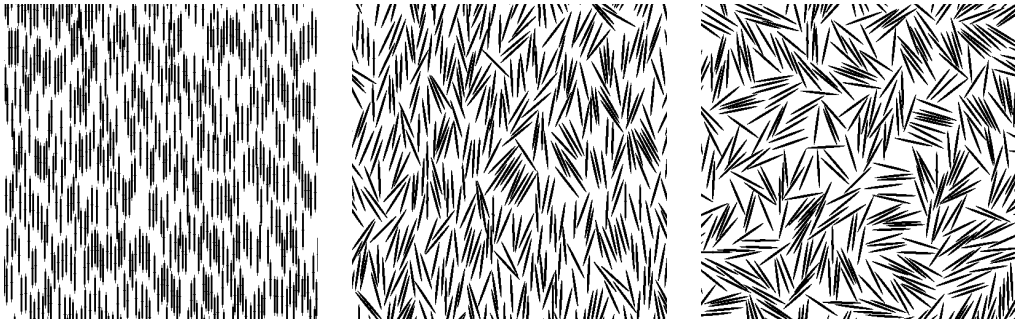

(a) 90° **(b)** 90° ± 20° **(c)** Random

Figure 2. The influence of orientation distribution on synthetic microstructures containing 30% area fraction second phase with a 16:1 aspect ratio. The 512 x 512 subimages show the alignment of particles in the (a) 90°, (b) 90° ± 20°, and (c) random orientation distributions.

[1]. Qualitatively, L_H for a particular microstructure is the length scale at which the variation between each sub-region becomes statistically indistinguishable from a larger area of material. In other words, L_H is the minimum length scale necessary to construct a volume element representative of a particular microstructure to a given degree of statistical confidence, typically selected to be 99.0% in the isotropic case.

The homogeneous length scale of a real or synthetic microstructure can be quantified by a technique termed the multi-scale analysis of area fractions (MSAAF) [1]. In this method, a digitized microstructure is re-sampled at various resolutions (corresponding to various length scales, Q_n) to determine the area fraction of a particular sub-region. Take for example, the first column of images in Fig. 3, where an initial microstructure is subdivided into 3 lower resolutions/length scales: Q_1, Q_2, Q_3. After subdivision, the effective area fraction (A_f) is assigned to each sub-region, visually depicted as a gray level in Fig. 3. By using all sub-regions available at a chosen length scale, an average area fraction and standard deviation (σ_{A_f}) in area fraction is determined for that Q_n. Though the average area fraction over all sub-regions for a particular length scale will not change with length scale, the standard deviation over all sub-regions will.

Consequently, the principal result of this technique is a plot depicting the evolution of the coefficient of variation (Ψ) - the ratio of standard deviation in second-phase area fraction to the global area fraction, σ_{A_f}/A_f - as a function of Q. Such a plot for the $20\%A_f$-$16AR$ condition is depicted in Fig. 4. When this plot decreases to a specified level of confidence (Ψ), the corresponding Q is termed the homogenous length scale (L_H). Differences in homogeneity between isotropic microstructures can be characterized using a value of L_H for each microstructure at a predetermined level of confidence [1]. For this reason, we use the isotropic MSAAF analysis of synthetic microstructures to characterize homogeneity with the 1% homogenous length scale, $L_H^{0.01}$, *i.e.*, the scale at which the variation in microstructure sub-region area fraction becomes less than 1% ($\Psi \leq 0.01$).

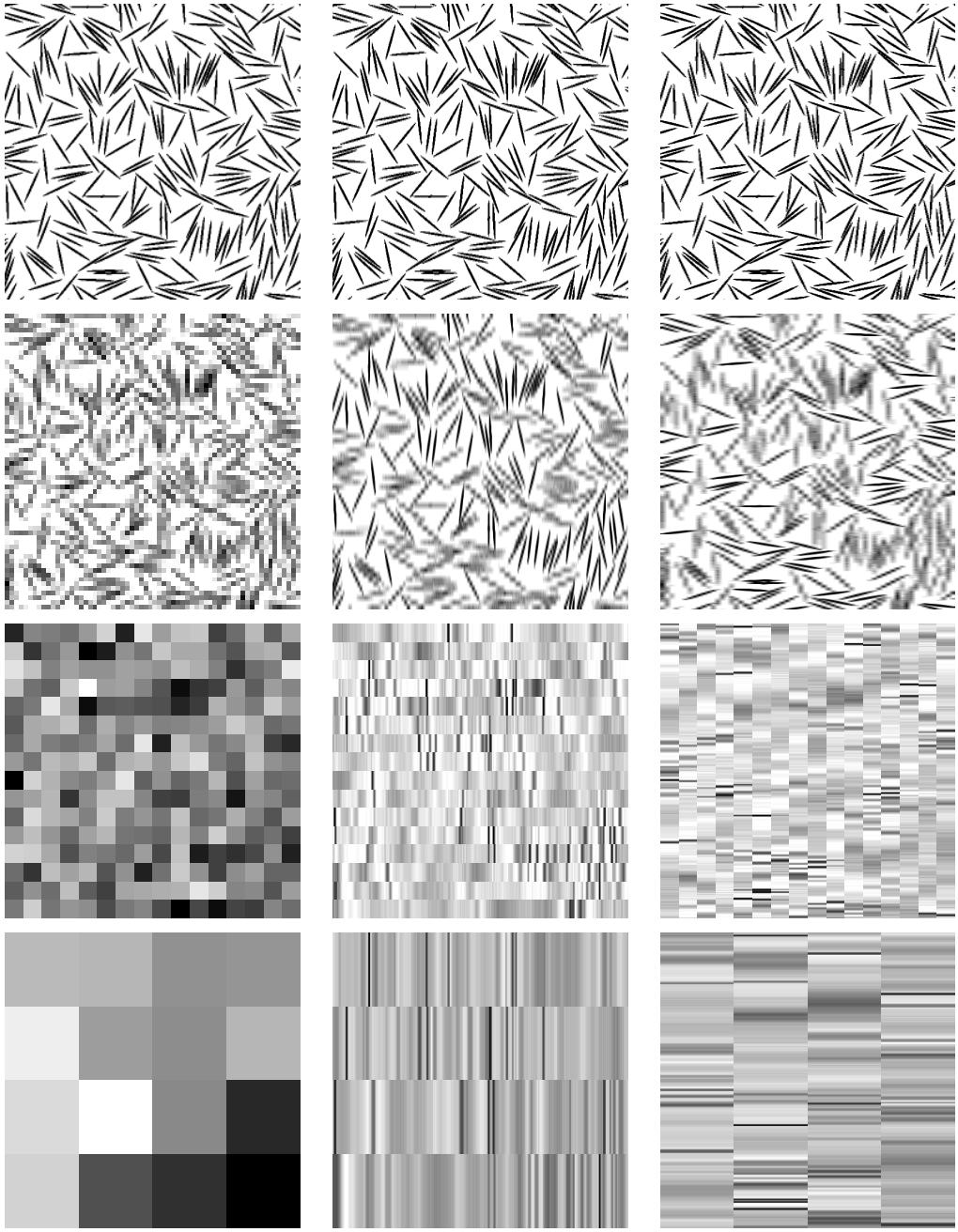

(a) Isotropic **(b)** Vertical **(c)** Horizontal

Figure 3. Evolution of the density area fraction of second phase (depicted by gray level) as a function of length scale Q according to the (a) isotropic MSAAF technique, as well as the directional technique applied in the (b) vertical and (c) horizontal directions for the synthesized $20\%A_f$-$16AR$ microstructure.

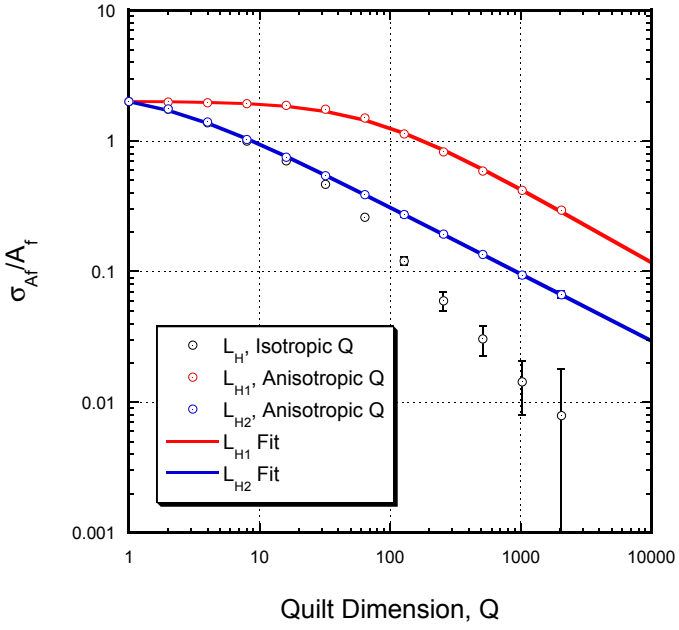

(a)

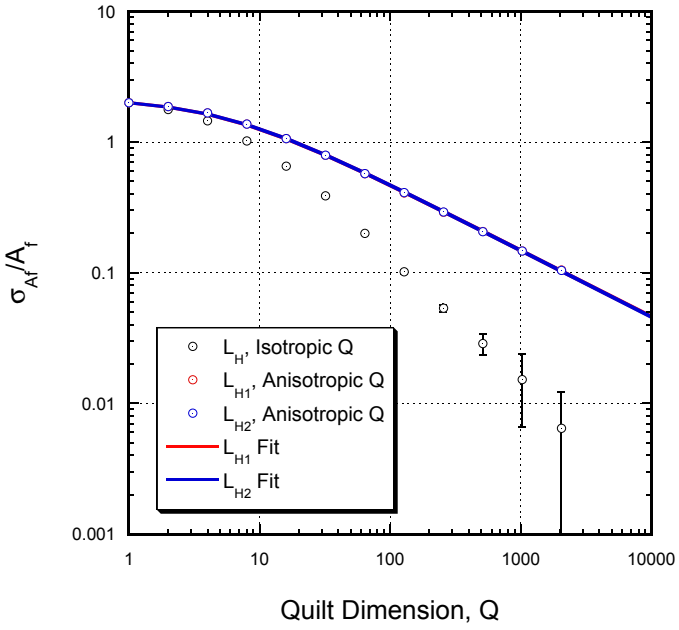

(b)

Figure 4. Isotropic and directional MSAAF plots for the synthesized 20%A_f-16AR microstructure with (a) aligned particles and (b) randomly oriented particles.

2.3.2. Anisotropic Microstructures When studying a area of material that is both anisotropic and inhomogeneous, it is useful to logically extend the concept of the homogenous length scale by measuring the *directional* variation in *linear* area fraction as a function of length scale to compute a *directional homogenous length scale*, L_{Hn}, where n is an integer index (valued from 1-3 for a 3-dimensional microstructure) denoting a principal particular (orthogonal) direction in the material [20]. Only a simple modification to the MSAAF technique is required to obtain values of L_{Hn} from plane sections of a material. As shown in the second and third columns of Fig. 3, rather than subdividing the microstructure into square elements, each line of pixels is subdivided into a number of strips for each corresponding length scale of interest (Q_n). The variation in area fraction of each of these strips is used to generate directional MSAAF plots (also depicted for the $20\%A_f$-$16AR$ in Fig. 4) to determine the orthogonal 10% ($\Psi = 0.1$) homogenous length scales, L_{H1} (vertical) and L_{H2} (horizontal). A value of $\Psi = 0.1$ (*i.e.*, 90% confidence) is chosen due to practical limitations on the sizes of images that can typically be obtained either experimentally or by simulation.

For all synthetic microstructure conditions resulting from the permutations of the factors in Table 1, the MSAAF technique and its directional counterpart were used to assess the influence of these factors on L_H, L_{H1}, and L_{H2}. Since the synthetic microstructure images are periodic, multiple instantiations of the same microstructure were sampled (by re-centering the image) to characterize the inherent variation in the isotropic and directional MSAAF techniques. To this end, 30 distinct instantiations of the same synthetic microstructure were used to calculate error values (3 standard deviations) at each length scale considered in the MSAAF analysis, as is also depicted by the error bars in Fig. 4.

3. Results and Discussion

3.1. Isotropic and Directional MSAAF Results

The isotropic homogenous length scale, $L_H(0.01)$, for different area fractions and aspect ratios of aligned particles (90° orientation distribution) is depicted in Fig. 5. First, as expected from previous work [14], there is a general decrease in L_H with increasing second phase area fraction. Second, there is seemingly no monotonic correlation between $L_H(0.01)$ and aspect ratio. Strongly contributing to this absence of correlation is the broad variation in $L_H(0.01)$ between different instantiations of each microstructure that often overlaps with adjacent conditions.

Directional homogenous length scales $L_{H1}(0.1)$ and $L_{H2}(0.1)$ for the aligned microstructures (90° orientation distributions) are depicted in Figs. 6(a) and 6(b), respectively. Here, trends with both area fraction and aspect ratio are apparent. Again, the inverse relationship between homogenous length scale and area fraction is clear. However, the directional length scale along the axis of alignment (L_{H1}) increases with aspect ratio while the opposite trend is observed in the transverse (L_{H2}) direction.

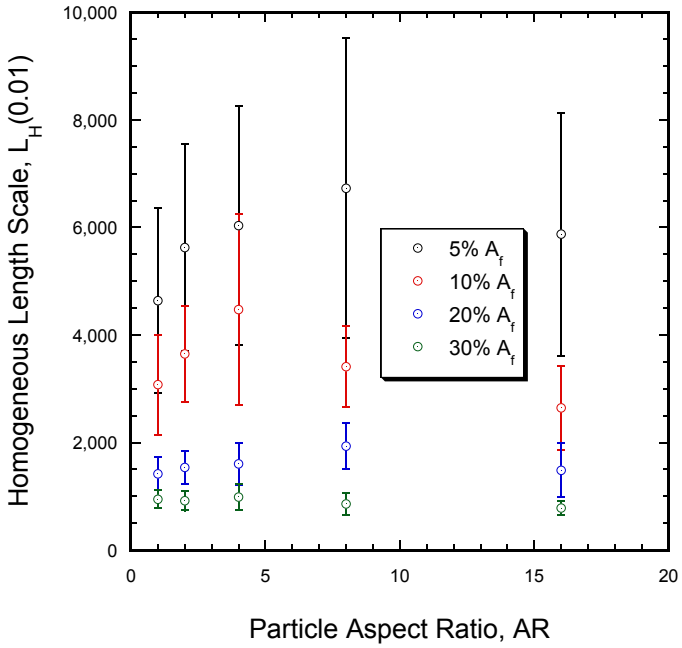

Figure 5. Isotropic homogenous length scale, $L_H(0.01)$, as a function of second-phase aspect ratio and area fraction for aligned (90° orientation distribution) particles; error bars represent the 3σ deviation from 30 instantiations of each condition.

Comparing Figs. 5 and 6 clearly indicates that for the isotropic MSAAF technique, error in L_H measurement can be significant when comparing orthotropic microstructures. This is due in part to the $(m-1)$ character of the standard deviation in area fraction used to compute Ψ, where m is the number of sub-regions; at large length scales, this deviation can influence the measurement of L_H. In contrast, the variation at each length scale resulting from the directional MSAAF technique is quite small since even at the largest length scale there are still 4096 sub-regions; the different length scales more accurately capture the contribution of orthotropy in the microstructure. For this reason, the terms containing fewer than 16 only 1 or 4 sub-regions are dropped when calculating the isotropic L_H to avoid including spurious values of L_H.

The effect of orientation distribution on the directional homogenous length scales as a function of aspect ratio for the synthetic microstructures containing $30\%A_f$ second phase is captured in Fig. 7. As expected, there is no difference in directional length scales for the random condition. However, the increasing propensity for second-phase alignment increases the separation of these orthogonal length scales by increasing L_{H1} and decreasing L_{H2}. This trend is characteristic of the other second phase area fractions as well.

3.2. Model for Homogenous Length Scales in Orthotropic Microstructures

MSAAF data has previously been fit [1] to an equation of the form

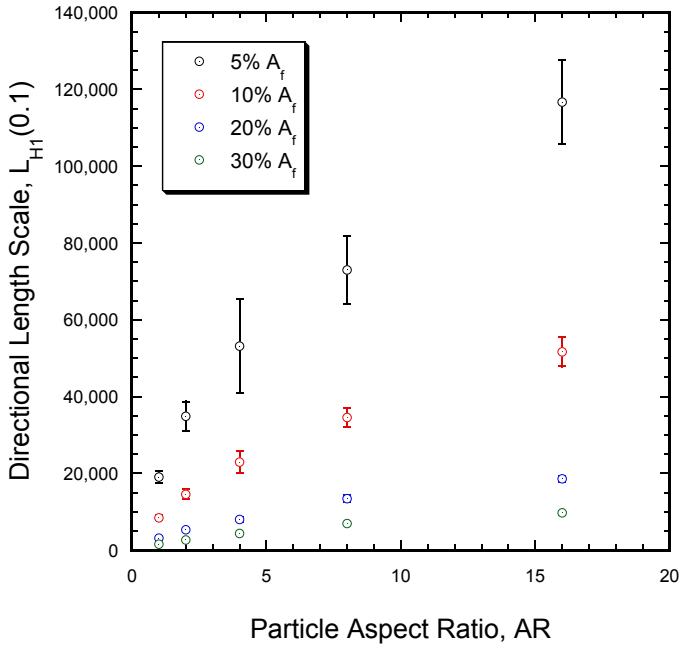

(a)

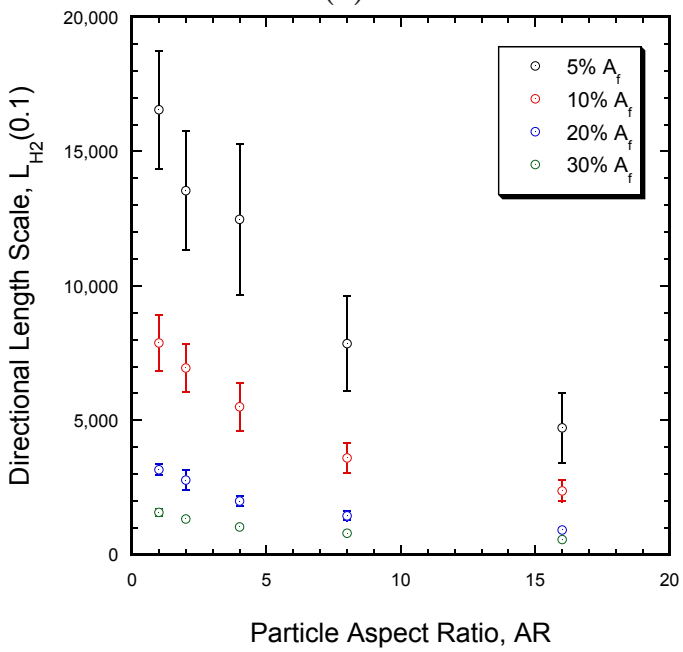

(b)

Figure 6. Directional homogeneous length scales, (a) $L_{H1}(0.1)$ and (b) $L_{H2}(0.1)$, as a function of second-phase aspect ratio and area fraction for aligned (90° orientation distribution) particles.

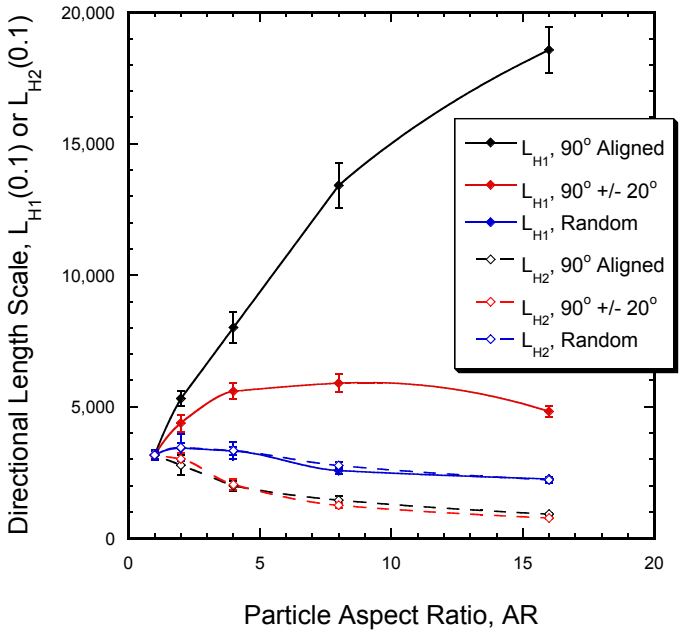

Figure 7. Directional homogenous length scales, $L_{H1}(0.1)$ and $L_{H2}(0.1)$, as a function of second-phase aspect ratio for random, semi-aligned, and aligned (90° orientation distribution) particles in a 30%A_f microstructure.

$$\Psi(A_f) = \frac{1}{\sqrt{A_f/(1-A_f) + \alpha {Q^*}^{-2\xi}}} \tag{1}$$

where α is a geometric factor related to particle size and area fraction, ξ is the slope of the long length-scale portion of the MSAAF plot, and Q^* is the discretized length scale (in pixels) [1]. In order to understand the effect of microstructure factors on homogenous length scales, least-squares fits to Eq. 1 were used to characterize the behavior of α and ξ for each synthetic microstructure condition. During such fits, it was observed that while $Q^* = Q$ fits MSAAF curves where α is small, large α values require $Q^* = Q - 1$. This is simply due to the discretized nature of the image, *i.e.*, the lower limit on Q is 1 pixel. This modification reflects that at a length scale of $Q = 1$, the coefficient of variation is entirely dependent on second phase area fraction (*i.e.*, $\Psi(A_f) = \sqrt{(1-A_f)/A_f}$). Use of this transformation for any α fully reconciles the short and long length-scale MSAAF behaviors originally proposed by Spowart et al. [1] and greatly improves the fit of Eq. 1 to MSAAF results, suggesting that the relationship

$$\Psi(A_f) = \frac{1}{\sqrt{A_f/(1-A_f) + \alpha (Q-1)^{-2\xi}}} \tag{2}$$

is more universal for discrete data than Eq. 1, particularly at short length scales.

The solid lines for the directional MSAAF plots shown in Fig. 4 are typical of fitting Eq. 2 to MSAAF results for all synthetic microstructures. Over all conditions $\xi_{isotropic} \approx -1$ and $\xi_{directional} \approx -0.5$, indicating that ξ is insensitive to all considered

Table 2. Coefficients for the a model of Eq. 3 for each Directional homogenous length scales, (a) L_{H1}, and (b) L_{H2} as a function of second-phase aspect ratio and area fraction for aligned (90° orientation distribution) particles.

Orientation	c_0	c_1	c_2	c_3	c_4
Random, L_{H1}	0.0201	0.2491	0.0117	0.0056	0.0327
Random, L_{H2}	0.0190	0.2682	0.0096	0.0058	0.0303
$90° \pm 20°$ Aligned, L_{H1}	-0.0049	0.1613	-0.0010	0.0024	0.0733
$90° \pm 20°$ Transverse, L_{H2}	0.0512	0.2267	0.0569	0.0090	-0.0066
90° Aligned, L_{H1}	-0.0091	0.0983	-0.0046	0.0006	0.0895
90° Transverse, L_{H2}	0.0583	0.2488	0.0570	0.0119	-0.0183

microstructure factors, as well as the method (isotropic or directional) used for characterizing homogeneity. On the other hand, α varied significantly with second phase area fraction, aspect ratio, and degree of alignment. Moreover, it has previously been shown [1] [11] that ξ can vary significantly with degree of clustering, although this was not studied in the present effort. Fig. 8 shows the evolution of α as function of second phase area fraction and aspect ratio for the (a) random orientation distribution, and the "perfectly" aligned orientation distribution in the (b) L_{H1} and (c) L_{H2} directions.

Inspecting the results for the random, partially aligned ($90° \pm 20°$), and "perfectly" aligned (90°) conditions showed that α obeys a relationship of the form

$$\alpha = A_f \left[c_0 + c_1 A_f + c_2 A_f AR + c_3 AR + c_4 \frac{1}{AR} \right] \tag{3}$$

where c_n are constants that are tabulated in Table 2 for each orientation distribution considered in this study. The quality of the fit from these coefficients to the calculated α values is depicted in Fig. 8(a)-(c) by the solid lines.

3.3. Implications for Representative Volume Elements Size in Orthotropic Materials

If it is assumed that $\xi = -0.5$, then Eq. 2 can be rearranged such that L_H, L_{H1}, and L_{H2} can be characterized by a relationship of the form

$$L_{Hn}^{\Psi} = \frac{1}{\alpha} \left[\frac{1}{\Psi^2} - \frac{A_f}{1 - A_f} \right] + 1 \cong \frac{1}{\alpha} \left[\frac{1}{\Psi^2} - \frac{A_f}{1 - A_f} \right] \tag{4}$$

where the index n of Eq. 4 is 1, 2, or 3 depending on the principal direction in the microstructure. Such an expression can then be used to estimate the size of a representative volume element for the considered orthotropic microstructures as a function of the second phase volume fraction (V_f), aspect ratio, and desired level of confidence (Ψ), *i.e.*,

$$V_{RVE}^{\Psi} = L_{H1}^{\Psi} L_{H2}^{\Psi} L_{H3}^{\Psi} = \frac{1}{\alpha_1 \alpha_2 \alpha_3} \left[\frac{1}{\Psi^2} - \frac{V_f}{1 - V_f} \right]^3 \tag{5}$$

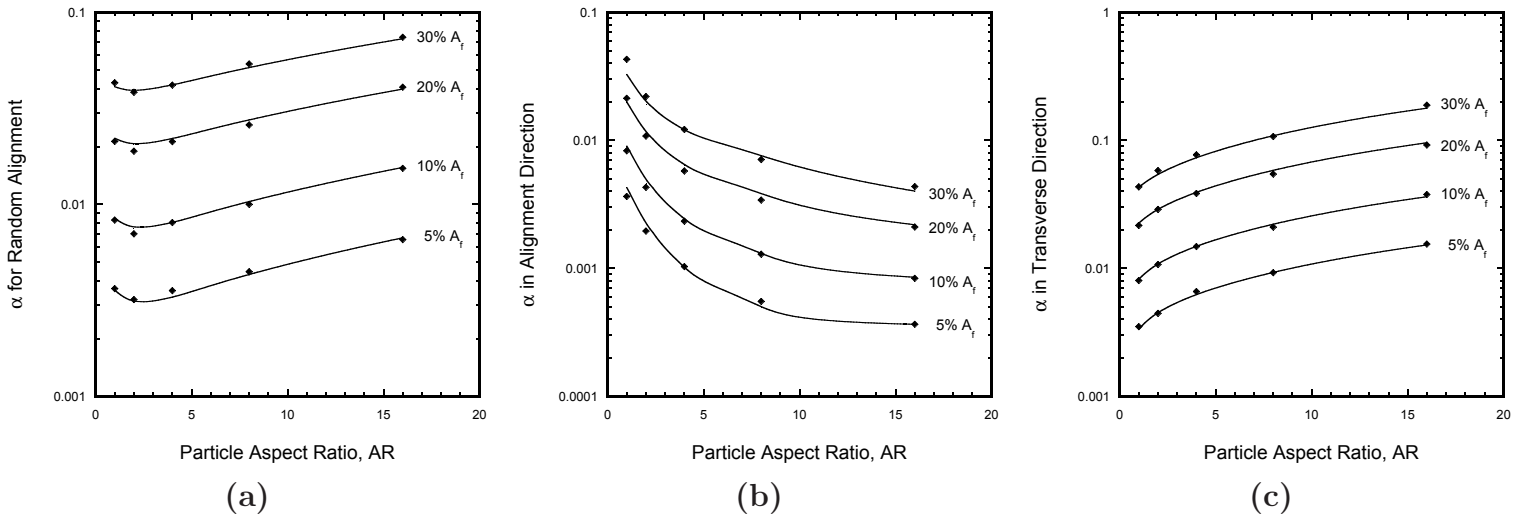

Figure 8. Evolution of the parameter α as a function of second phase area fraction and aspect ratio for (a) random and "perfectly" aligned (90°) orientation distributions in the (b) $L_{H1}(0.1)$ and (c) $L_{H2}(0.1)$ directions.

If symmetry is maintained about the axis of alignment (the 1 direction) and the second phase is needle-shaped not disc-shaped, then $\alpha_2 = \alpha_3$ and the size of the RVE necessary to characterize the 3-dimensional variants of the orthotropic microstructures can be determined as a function of the factors considered in this work. To that end, Fig. 9(a-c) captures the effect of second phase volume fraction and aspect ratio on RVE size for the (a) random, (b) $90° \pm 20°$, and (c) "perfectly" (90°) aligned orientation distributions.

4. Discussion

There are a few caveats of the 2D synthetic microstructures generated in this work. The random placement of particles may not be entirely representative of extrusion or directional synthesis processing. For example, the nearest neighbor separation could contract during extrusion in addition to second phase alignment or there could be alignment of second phase centroids in addition to the orientation of the principal axis. In this respect, the methodology for generating synthetic microstructures could be altered to better represent the microstructure within a specific material processed in a specific manner, *i.e.*, two-point correlation functions of experimental microstructures could be used to generate statistically-similar synthetic microstructures [24, 25, 26, 27, 28, 29, 30]. Additionally, there are many aspects of microstructures in real materials that have not been explored in the current work, *i.e.*, particle morphology (in addition to aspect ratio), particle size distribution, and particle clustering (spatial distribution), to name a few. We leave these microstructure-specific aspects of second phase particles for future work.

Nevertheless, by controlling the second-phase particle alignment, aspect ratio, and area fraction when generating the 2D periodic synthetic microstructures, the following work illuminates how the computationally-efficient MSAAF technique can be used for understanding the inherent alignment of second phase particles in *experimental* images. The two microstructure parameters, α and ξ, used for fitting Eq. 2 represent the evolution of the variation in area fraction as a function of length scale. The directional and homogeneous length scales from the MSAAF technique signify a quantitative metric for characterizing the representative length scale or volume element for a given microstructure. The significance of this work is that the analysis of experimental images with the MSAAF technique can be compared and interpreted based on the results of various synthetic microstructures examined in this work.

Future work will encompass generating 3D periodic synthetic microstructures with second phase particles of known sizes, aspect ratios, and orientations; analyzing 2D orthogonal slices may help our understanding of how quantitative information informed from 2D orthogonal slices relates to the known 3D structure. This will test the validity of stereological assumptions often employed for relating 2D microstructural information to 3D volumes [31]. Additional work will concentrate on generating synthetic microstructures with various degrees of particle clustering to improve our understanding of how clustering impacts the representative length scales of realistic microstructures.

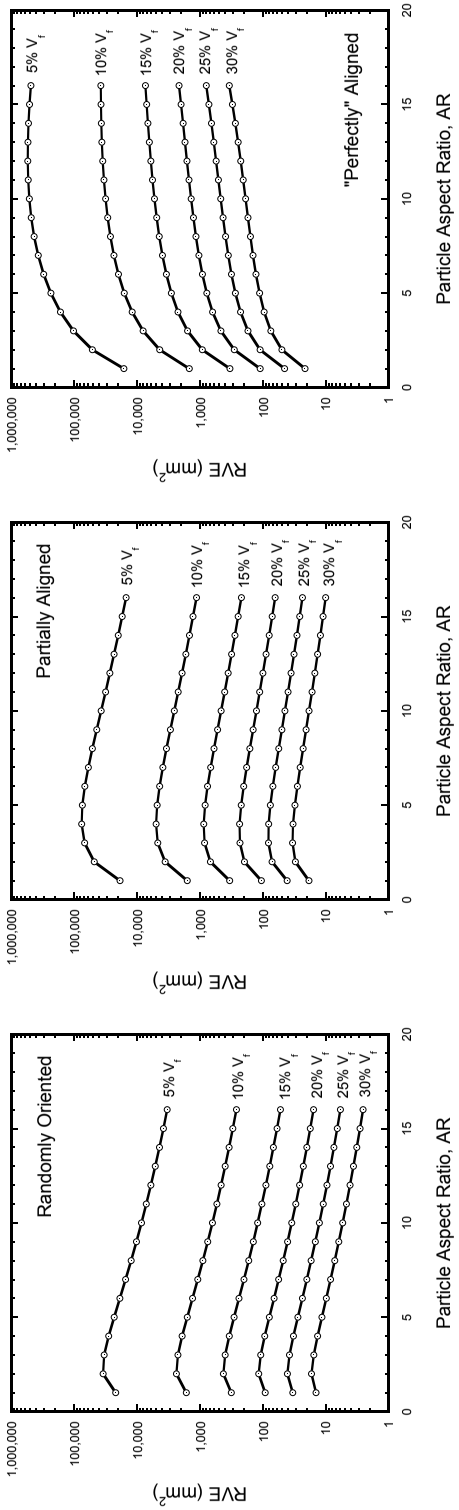

Figure 9. Effect of second phase area volume fraction (A_f) and aspect ratio (AR) on 2-dimensional RVE size for the (a) random, (b) $90° \pm 20°$, and (c) "perfectly" (90°) aligned orientation distributions.

Also, as shown in the present work, the directional length scale indicates alignment (or non-alignment) in a particular direction; by applying the directional MSAAF technique along multiple orientations, the associated alignment texture of second-phase particles within a microstructure image can be easily ascertained.

5. Summary

In this work, synthetic two-phase microstructures with known area fractions, aspect ratios, and orientations of second phase particles were generated to probe the effects of orthotropy on metrics used to measure representative length scales: the isotropic and directional homogenous length scales calculated from the Multi-Scale Analysis of Area Fractions (MSAAF) technique. The prime result of this work is a template for determining the representative length scale (and volume) of microstructure in a given 2D section as a function of specific microstructure factors (area fraction, aspect ratio, alignment propensity). Ancillary results of this work are:

(i) The calculated standard deviation (error) from 30 instantiations of each periodic synthetic microstructure is substantially lower for directional homogenous length scales when compared with the isotropic homogenous length scale. This is attributable to the number of constituent subdivisions of an image at larger length scales. Therefore, to avoid this deviation the extent of the domain must be large compared to the representative length scale being measured; this is especially important for the isotropic MSAAF technique.

(ii) The directional MSAAF technique is useful for characterizing the relative alignment of second phase particles in the synthetic microstructures generated. The deviation between the directional length scales in two orthogonal directions increases as a function of particle alignment and aspect ratio. The homogeneous and directional length scales increase with decreasing area fraction of particles.

The present work shows how the isotropic and directional MSAAF techniques can help quantitatively characterize orthotropic microstructures with second phase particles of varying alignments.

Acknowledgments

This work is a complement to GBW's dissertation, which was supported through funding from the Air Force Office of Scientific Research (Grant # 01ML05-COR, Program Manager Dr. Joan Fuller).

References

[1] J.E. Spowart, B. Maruyama, and D.B. Miracle. Multi-scale characterization of spatially heterogeneous systems: Implications for discontinuously reinforced metal-matrix composite microstructures. *Mater. Sci. Eng. A*, 307:51 – 66, 2001.

[2] A. Borbely, P. Kenesei, and H. Biermann. Estimation of the effective properties of particle-reinforced metal matrix composites from microtomographic reconstructions. *Acta Mater.*, 54:2735 – 2744, 2006.

[3] Binglin Lu and S. Torquato. Local volume fraction fluctuations in heterogeneous media. *J. Chem. Phys.*, 93:3452 – 3459, 1990.

[4] J. Quintanilla and S. Torquato. Local volume fraction fluctuations in random media. *J. Chem. Phys.*, 106:2741 – 2751, 1997.

[5] M. Li, S. Ghosh, O. Richmond, H. Weiland, and T.N. Rouns. Three dimensional characterization and modeling of particle reinforced metal matrix composites: Pt. I. Quantitative description of microstructural morphology. *Mater. Sci. Eng. A*, 265:153 – 173, 1999.

[6] M. Li, S. Ghosh, O. Richmond, H. Weiland, and T.N. Rouns. Three dimensional characterization and modeling of particle reinforced metal matrix composites part II: Damage characterization. *Mater. Sci. Eng. A*, 266:221 – 240, 1999.

[7] P. Louis and A.M. Gokhale. Computer simulation of spatial arrangement and connectivity of particles in three-dimensional microstructure: Application to model electrical conductivity of polymer matrix composite. *Acta Mater.*, 44:1519 – 1528, 1996.

[8] Zhaohui Shan and Arun M. Gokhale. Representative volume element for non-uniform microstructure. *Comp. Mater. Sci.*, 24:361 – 379, 2002.

[9] Somnath Ghosh, D.M. Valiveti, Stephen J. Harris, and James Boileau. A domain partitioning based pre-processor for multi-scale modelling of cast aluminium alloys. *Modelling Simul. Mater. Sci. Eng.*, 14:1363 – 1396, 2006.

[10] D.M. Valiveti and Somnath Ghosh. Morphology based domain partitioning of multi-phase materials: A preprocessor for multi-scale modelling. *Int. J. Numer. Meth. Eng.*, 69:1717 – 1754, 2007.

[11] J.E. Spowart. Microstructural characterization and modeling of discontinuously-reinforced aluminum composites. *Mater. Sci. Eng. A*, 425:225 – 237, 2006.

[12] K. Faber and A. Evans. Crack deflection process I. Theory. *Acta Metall.*, 31:565 – 576, 1983.

[13] K. Faber and A. Evans. Crack deflection process II. Experiment. *Acta Metall.*, 31:577 – 584, 1983.

[14] G.B. Wilks. *Influence of Reinforcement Homogeneity on the Deformation and Fracture of a Discontinuously Reinforced Aluminum Matrix Composite*. PhD thesis, Pennsylvania State University, 2007.

[15] H. Kumar, C.L. Briant, and W.A. Curtin. Using microstructure reconstruction to model mechanical behavior in complex microstructures. *Mech. Mater.*, 38:818 – 832, 2006.

[16] Somnath Ghosh, J. Bai, and P. Raghavan. Concurrent multi-level model for damage evolution in microstructurally debonded composites. *Mech. Mater.*, 39:241 – 266, 2007.

[17] S. Yang and A.M. Gokhale Application of image processing for simulation of mechanical response of multi-length scale microstructures of engineering alloys. *Metall. Mater. Trans. A*, 30:2369 – 2381, 1999.

[18] Z. Shan and A.M. Gokhale. Micromechanics of complex three-dimensional microstructures. *Acta Mater.*, 49:2001 – 2015, 2001.

[19] A. Ayyar and N. Chawla. Microstructure-based modeling of crack growth in particle reinforced composites. *Composites Sci. Tech.*, 66:1980 – 1994, 2006.

[20] A. Tewari, A.M. Gokhale, J.E. Spowart, and D.B. Miracle. Quantitative characterization of spatial clustering in three-dimensional microstructures using two-point correlation functions. *Acta Mater.*, 52:307 – 19.

[21] A. Cadilhe, N.A.M. Araujo, and V. Privman. Random sequential adsorption: from continuum to lattice and pre-patterned substrates. *J. Phys.*, 19:065124, 2007.

[22] V.A. Buryachenko, N.J. Pagano, R.Y. Kim, and J.E. Spowart. Quantitative description and numerical simulation of random microstructures of composites and their effective elastic moduli. *Int. J. Solids Struct.*, 40:47 – 72, 2003.

[23] E.L. Hinrichsen, J. Feder, and T. Jossang. Geometry of random sequential adsorption. *J. Stat. Phys.*, 44:793 – 822, 1986.

[24] H. Singh, A.M. Gokhale, Y. Mao, and J.E. Spowart. Computer simulations of realistic microstructures of discontinuously reinforced aluminum alloy (DRA) composites. *Acta Mater.*, 54:2131 – 2143, 2006.

[25] H. Singh, Y. Mao, A. Sreeranganathan, and A.M. Gokhale. Application of digital image processing for implementation of complex realistic particle shapes/morphologies in computer simulated heterogeneous microstructures. *Modelling Simul. Mater. Sci. Eng.*, 14:351 – 63, 2006.

[26] N. Sheehan and S. Torquato. Generating microstructures with specified correlation functions. *J. Appl. Phys.*, 89:53 – 60, 2001.

[27] C. L. Y. Yeong and S. Torquato. Reconstructing random media. *Phys. Rev. E*, 57:495–506, 1998.

[28] C. L. Y. Yeong and S. Torquato. Reconstructing random media. II. Three-dimensional media from two-dimensional cuts. *Phys. Rev. E*, 58:224–233, 1998.

[29] Y. Jiao, F.H. Stillinger, and S. Torquato. Modeling heterogeneous materials via two-point correlation functions: Basic principles. *Phys. Rev. E*, 76:031110, 2007.

[30] Y. Jiao, F.H. Stillinger, and S. Torquato. Modeling heterogeneous materials via two-point correlation functions: II. Algorithmic details and applications. *Phys. Rev. E*, 77:031135, 2008.

[31] E. E. Underwood. *Quantitative Stereology.* Addison-Wesley, Reading, MA, 1970.